

Mechanism in Polyoxometalate-Catalyzed Homogeneous Hydrocarbon Oxo Transfer Oxidation. The $[\text{Co}_4(\text{H}_2\text{O})_2\text{P}_2\text{W}_{18}\text{O}_{68}]^{10-}$ -*p*-Cyano-*N,N*-dimethylaniline *N*-Oxide Selective Catalytic Epoxidation System

Xuan Zhang, Ken Sasaki, and Craig L. Hill*

Contribution from the Department of Chemistry, Emory University, Atlanta, Georgia 30322

Received November 2, 1995[⊗]

Abstract: The Co-substituted heteropolyanions $[\text{Co}_4\text{P}_2\text{W}_{18}\text{O}_{68}]^{10-}$ and $[\text{CoPW}_{11}\text{O}_{39}]^{5-}$ catalyze the highly selective epoxidation of disubstituted alkenes and stilbenes by *p*-cyano-*N,N*-dimethylaniline *N*-oxide (CDMANO). Terminal alkenes are not readily epoxidized. The following d-electron transition metal-substituted (TMSP) complexes are less selective and two orders of magnitude less reactive than the Co complexes: $[\text{Mn}^{\text{III}}\text{PW}_{11}\text{O}_{39}]^{4-}$, $[\text{Mn}^{\text{II}}\text{PW}_{11}\text{O}_{39}]^{5-}$, $[\text{Fe}^{\text{III}}\text{PW}_{11}\text{O}_{39}]^{4-}$, and $[\text{Ni}^{\text{II}}\text{PW}_{11}\text{O}_{39}]^{5-}$. The system $(\text{TBA})_8\text{H}_2[\text{Co}_4\text{P}_2\text{W}_{18}\text{O}_{68}]$ ($\text{TBA} = n\text{-Bu}_4\text{N}^+$) (TBA1)/CDMANO/alkene/ CH_3CN solvent is homogeneous throughout. The values for K_1 (constant for 1:1 association of the following ligands with **1** under the catalytic conditions in these studies = acetonitrile solution, 25 or 50 °C) are 275 ± 13 (*N*-methylimidazole), 4.3 ± 0.1 (pyridine), 59 ± 3 (4-picoline *N*-oxide), 22 ± 1 (4-cyanopyridine *N*-oxide), and 57 ± 5 (*N*-methylmorpholine *N*-oxide, MMNO, a model for CDMANO). Comparisons of the electronic absorption spectra of **1** under catalytic turnover and several other conditions indicate formation of the 1:1 CDMANO adduct, a result also consistent with thermodynamic binding and kinetic data. Chromatographic separation and spectral (UV–visible, NMR) evidence indicate that the brown color in the epoxidation reactions evident after many turnovers results from condensed heterocyclic structures from oxidation of the principal product derived from CDMANO during catalysis, *p*-cyano-*N,N*-dimethylaniline (CDMA). Evaluation of the kinetics of cyclohexene epoxidation by CDMANO over a wide range of conditions affords the following empirical rate law: $\{d[\text{epoxide}]/dt\}_{\text{initial}} = k'[\text{cyclohexene}]_i[\text{CDMANO}]_i[\mathbf{1}]_{\text{total}}/(k''[\text{CDMANO}]_i + k'''[\text{cyclohexene}]_i + k''''[\text{cyclohexene}]_i[\text{CDMANO}]_i + k''''')$. This is inconsistent with several common catalytic oxygenation mechanisms but consistent with a three-step mechanism: an initial pre-equilibrium association of **1** and CDMANO; loss of CDMA and formation of a reactive high-valent cobalt intermediate; and then transfer of oxygen from the intermediate to alkene.

Introduction

The versatility, accessibility, and low toxicity of early transition metal oxygen anion clusters, polyoxometalates for short, have led to many recent applications of these compounds in catalysis, medicine, and materials science.^{1–14} The d^0 electronic configuration of many polyoxometalates including heteropolyanions render them oxidatively resistant and hence particularly attractive as homogeneous and heterogeneous oxidation catalysts.^{9–12,14} The substitution of one or more of

the skeletal d^0 (usually W^{VI}) ions in many heteropolyanions with d-electron transition metal ion(s) of the appropriate redox potential and electronic properties affords oxidation catalysts that can function as oxidatively resistant analogs of metalloporphyrins. These d-electron transition metal substituted polyoxometalate (TMSP) complexes can combine the selectivity advantages of homogeneous catalysts such as metalloporphyrins with the stability advantages of conventional heterogeneous metal oxide oxidation catalysts. Since the first oxygenation catalysis by a TMSP complex,¹⁵ ~50 papers have addressed the oxygenation or oxidation of a variety of substrates including alkanes and alkenes^{16–29} and this literature has just been comprehensively reviewed.¹⁴

[⊗] Abstract published in *Advance ACS Abstracts*, May 1, 1996.

(1) Pope, M. T. *Heteropoly and Isopoly Oxometalates*; Springer-Verlag: Berlin, 1983.

(2) Day, V. W.; Klemperer, W. G. *Science* **1985**, *228*, 533–541.

(3) Pope, M. T.; Müller, A. *Angew. Chem., Int. Ed. Engl.* **1991**, *30*, 34–48.

(4) Chen, Q.; Zubieta, J. *Coord. Chem. Rev.* **1992**, *114*, 107–167.

(5) Saha, S. K.; Ali, M.; Banerjee, P. *Coord. Chem. Rev.* **1993**, *122*, 41–62.

(6) Kozhevnikov, I. V. *Russ. Chem. Rev.* **1993**, *62*, 473–491.

(7) Hill, C. L.; Prosser-McCartha, C. M. In *Photosensitization and Photocatalysis Using Inorganic and Organometallic Complexes*; Kalyanasundaram, K.; Grätzel, M., Eds.; Kluwer Academic Publishers: Dordrecht, The Netherlands, 1993; Vol. 14, Chapter 13, pp 307–330.

(8) Hill, C. L.; Kim, G.-S.; Prosser-McCartha, C. M.; Judd, D. *Mol. Eng.* **1993**, *3*, 263–275.

(9) Okuhara, T.; Misono, M. *Yuki Gosei Kagaku Kyokaiishi* **1993**, *51*, 128–140.

(10) Mizuno, N.; Misono, M. *J. Mol. Catal.* **1994**, *86*, 319–342.

(11) Jansen, R. J. J.; Vanveldhuizen, H. M.; Schwegler, M. A.; Vanbekkum, H. *Recl. Trav. Chim. Pays-Bas* **1994**, *113*, 115–135.

(12) Kozhevnikov, I. V. *Catal. Rev.-Sci. Eng.* **1995**, *37*, 311–352.

(13) Maksimov, G. M. *Usp. Khim.* **1995**, *64*, 480–496.

(14) Hill, C. L.; Prosser-McCartha, C. M. *Coord. Chem. Rev.* **1995**, *143*, 407–455.

(15) Hill, C. L.; Brown, R. B., Jr. *J. Am. Chem. Soc.* **1986**, *108*, 536–538.

(16) Rong, C.; Pope, M. T. *J. Am. Chem. Soc.* **1992**, *114*, 2932–2938.

(17) Mansuy, D.; Bartoli, J.-F.; Battioni, P.; Lyon, D. K.; Finke, R. G. *J. Am. Chem. Soc.* **1991**, *113*, 7222–7226.

(18) Steckhan, E.; Kandzia, C. *Synlett* **1992**, 139–140.

(19) Bressan, M.; Morvillo, A.; Romanello, G. *J. Mol. Catal.* **1992**, *77*, 283–288.

(20) Khenkin, A. M.; Duncan, D. C.; Hill, C. L. *J. Am. Chem. Soc.* In submission.

(21) Khenkin, A. M.; Hill, C. L. *Mendeleev Commun.* **1993**, 140–142.

(22) Khenkin, A. M.; Hill, C. L. *J. Am. Chem. Soc.* **1993**, *115*, 8178–8186.

(23) Toth, J. E.; Anson, F. C. *J. Am. Chem. Soc.* **1989**, *111*, 2444–2451.

(24) Schwegler, M.; Floor, M.; van Bekkum, H. *Tetrahedron Lett.* **1988**, *29*, 823–826.

(25) Neumann, R.; Gara, M. *J. Am. Chem. Soc.* **1995**, *117*, 5066–5074.

(26) Neumann, R.; Khenkin, A. M.; Dahan, M. *Angew. Chem., Int. Ed. Engl.* **1995**, *34*, 1587–1589.

The complexity of these homogeneous TMSP-catalyzed oxidation systems has rendered the acquisition of quantitative rate and mechanistic information difficult. All the oxidants used to date, iodosylarenes, alkylhydroperoxides, hydrogen peroxide, periodate, and others have intrinsic limitations. Transition metal catalyzed oxidations by iodosylarenes can lead to substrate oxidation and oxygenation not involving intermediate high-valent oxometal species (iodine based radicals and/or metal bound iodosylarene units)^{30–32} and the polymeric nature of the oxidant militates against the acquisition of meaningful kinetics data.³³ At the same time, quantitative kinetics studies (rate constants, etc.) in transition metal catalyzed oxidations by alkyl hydroperoxides and hydrogen peroxide are usually compromised by the presence of Haber Weiss and other oxy radical based oxidation processes.^{34–37} Several kinetically competent oxidizing intermediates derived from the starting oxidant can also be important in peroxide and periodate oxidations. In the one TMSP-catalyzed oxygenation system involving a well-defined active oxygen transferring intermediate, hydrocarbon oxygenation by PhIO, *t*-BuOOH, and H₂O₂ catalyzed by isolable oxoCr^V Keggin species, catalysis is very sluggish.²² We have turned to reactive *N*-oxides in this study to design a TMSP-catalyzed hydrocarbon oxidation system that is fast and yet remains as simple and kinetically tractable as possible to facilitate a deeper elucidation of mechanism. The tractability of reactive *N*-oxides facilitated acquisition of a wealth of information, largely by Bruce and co-workers, on biomimetic metalloporphyrin-catalyzed oxidation reactions.^{38–46}

We report here the homogeneous oxidation of alkenes by *p*-cyano-*N,N*-dimethylaniline *N*-oxide (CDMANO) catalyzed by several TMSP complexes, with those catalyzed by [Co₄P₂W₁₈O₆₈]^{10–}, **1**, and [CoPW₁₁O₃₉]^{5–} being highly selective for epoxide. The stoichiometry of the epoxidation process, like that in the porphyrin studies, is that given in eq 1.^{38–46} The epoxidation has been investigated by association equilibria of intermediate species, spectroscopic examination of oxygen donor–catalyst complexes under catalytic conditions, and

(27) Neumann, R.; Dahan, M. *J. Chem. Soc., Chem. Commun.* **1995**, 171–172.

(28) Neumann, R.; Gara, M. *J. Am. Chem. Soc.* **1994**, *116*, 5509–5510.

(29) Bart, J. C.; Anson, F. C. *J. Electroanal. Chem.* **1995**, *390*, 11–19.

(30) Yang, Y.; Diederich, F.; Valentine, J. S. *J. Am. Chem. Soc.* **1990**, *112*, 7826–7828.

(31) Smegal, J. A.; Schardt, B. C.; Hill, C. L. *J. Am. Chem. Soc.* **1983**, *105*, 3510–3515.

(32) Smegal, J. A.; Hill, C. L. *J. Am. Chem. Soc.* **1983**, *105*, 3515–3521.

(33) Schardt, B. C.; Hill, C. L. *Inorg. Chem.* **1983**, *22*, 1563–1565.

(34) Sheldon, R. A.; Kochi, J. K. *Metal-Catalyzed Oxidations of Organic Compounds*; Academic Press: New York, 1981; Chapter 3.

(35) Hill, C. L.; Khenkin, A. M.; Weeks, M. S.; Hou, Y. In *ACS Symposium Series on Catalytic Selective Oxidation*; Oyama, S. T., Hightower, J. W., Eds.; American Chemical Society: Washington, DC, 1993; Chapter 6, pp 67–80.

(36) Drago, R. S.; Beer, R. H. *Inorg. Chim. Acta* **1992**, *200*, 359–367.

(37) Drago, R. S. *Coord. Chem. Rev.* **1992**, *117*, 185–213.

(38) Dicken, C. M.; Lu, F.-L.; Nee, M. W.; Bruce, T. C. *J. Am. Chem. Soc.* **1985**, *107*, 5776–5789.

(39) Yuan, L.-C.; Calderwood, T. S.; Bruce, T. C. *J. Am. Chem. Soc.* **1985**, *107*, 8273–8274.

(40) Dicken, C. M.; Woon, T. C.; Bruce, T. C. *J. Am. Chem. Soc.* **1986**, *108*, 1636–1643.

(41) Woon, T. C.; Dicken, C. M.; Bruce, T. C. *J. Am. Chem. Soc.* **1986**, *108*, 7990–7995.

(42) Dicken, C. M.; Lu, F.-L.; Bruce, T. C. *Tetrahedron Lett.* **1986**, *27*, 5967–5970.

(43) Wong, W.-H.; Ostovic, D.; Bruce, T. C. *J. Am. Chem. Soc.* **1987**, *109*, 3428–3436.

(44) Bruce, T. C.; Dicken, C. M.; Balasubramanian, P. N.; Woon, T. C.; Lu, F.-L. *J. Am. Chem. Soc.* **1987**, *109*, 3436–3443.

(45) Ostovic, D.; Knobler, C. B.; Bruce, T. C. *J. Am. Chem. Soc.* **1987**, *109*, 3444–3451.

(46) Dicken, C. M.; Balasubramanian, P. N.; Bruce, T. C. *Inorg. Chem.* **1988**, *27*, 197–200.

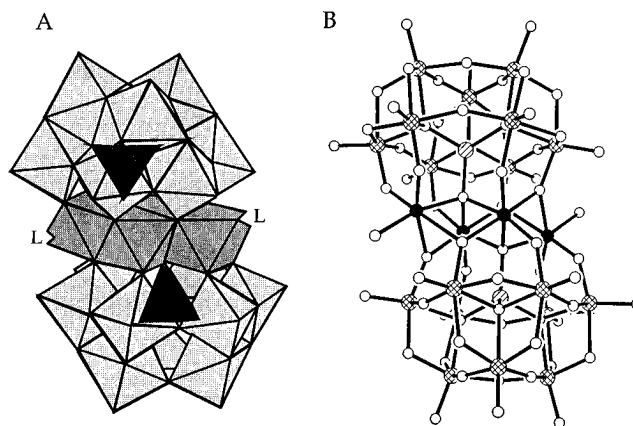


Figure 1. Structure of **1**. (A) Polyhedron illustration. The two P^V heteroatoms are the dark tetrahedra in the middle of the upper and lower PW₉ units. The four Co^{II} ions are the four darker edge-sharing octahedra in the middle of the structure. (B) Ball and stick illustration. The two P^V heteroatoms are the striped spheres in the middle of the upper and lower PW₉ units. The four Co^{II} ions are the black spheres in the middle of the structure.



evaluations of kinetic dependence of all reaction components on the rate. An illustration of **1**, a structural class of polytungstophosphates first reported by Weakley, Tourné, and co-workers⁴⁷ and studied by several groups since,^{21,48–55} is depicted in Figure 1.

Experimental Section

Materials and Methods. The potassium salts of transition metal substituted polyoxotungstate derivatives K_{5,4}[M^{II,III}PW₁₁O₃₉] (M = Co^{II}, Mn^{II}, Mn^{III}, Ni^{II}, Fe^{II}, Fe^{III})⁵⁶ and K₁₀[M₄(H₂O)₂(PW₉O₃₄)₂] (M = Co^{II}, Mn^{II}, Fe^{II}, Ni^{II})⁴⁹ and the tetra-*n*-butylammonium (⁴Q) salts of ⁴Q_{5,4}[M^{II,III}PW₁₁O₃₉]⁵⁷ were prepared and purified by literature methods. The purity of the compounds was checked by IR or/and ³¹P NMR. Acetonitrile (B&J) and methylene chloride (B&J) were dried over 3 Å molecular sieves under argon. All other chemicals were the best available reagent grade and were used without further purification. *p*-Cyano-*N,N*-dimethylaniline *N*-oxide (CDMANO) was prepared by the method of Craig and Purushothaman⁵⁸ and recrystallized from acetone–petroleum ether under nitrogen. CDMANO was dried under vacuum for 10 h before use and stored in a desiccator in the refrigerator. The reaction with hydrated CDMANO gave slower rates and less reproducible data.

(47) Weakley, T. J. R.; Evans, H. T., Jr.; Showell, J. S.; Tourné, G. F.; Tourné, C. M. *J. Chem. Soc., Chem. Commun.* **1973**, 139–140.

(48) Finke, R. G.; Droegge, M.; Hutchinson, J. R.; Gansow, O. *J. Am. Chem. Soc.* **1981**, *103*, 1587–1589.

(49) Finke, R. G.; Droegge, M.; Domaille, P. *J. Inorg. Chem.* **1987**, *26*, 3886–3896.

(50) Weakley, T. J. R.; Finke, R. G. *Inorg. Chem.* **1990**, *29*, 1235–1241.

(51) Gómez-García, C. J.; Casañ-Pastor, N.; Coronado, E.; Baker, L. C. W.; Pourroy, G. *J. Appl. Phys.* **1990**, *67*, 5995–5997.

(52) Gómez-García, C. J.; Coronado, E.; Borrassalmenar, J. J. *Inorg. Chem.* **1992**, *31*, 1667–1673.

(53) Casañ-Pastor, N.; Bas-Serra, J.; Coronado, E.; Pourroy, G.; Baker, L. C. W. *J. Am. Chem. Soc.* **1992**, *114*, 10380–10383.

(54) Gómez-García, C. J.; Borrassalmenar, J. J.; Coronado, E.; Delhaes, P.; Garrigoulafrange, C.; Baker, L. C. W. *Synth. Met.* **1993**, *56*, 2023–2027.

(55) Gómez-García, C. J.; Coronado, E.; Gómez-Romero, P.; Casañ-Pastor, N. *Inorg. Chem.* **1993**, *32*, 3378–3381.

(56) Malik, S. A.; Weakley, T. J. R. *J. Chem. Soc. A* **1968**, 2647–2650.

(57) Tourné, C. R.; Tourné, G. F.; Malik, S. A.; Weakley, T. J. R. *J. Inorg. Nucl. Chem.* **1970**, *32*, 3875–3881.

(58) Craig, J. C.; Purushothaman, K. K. *J. Org. Chem.* **1970**, *35*, 1721–1722.

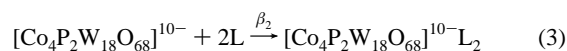
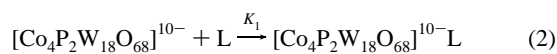
Instrumentation. The organic products were identified and quantified by gas chromatography (GC; Hewlett-Packard 5890 gas chromatograph equipped with a flame ionization detector and a 5% phenyl methyl silicone capillary column with nitrogen as a carrier gas) and gas chromatography/mass spectrometry (GC/MS; Hewlett-Packard 5890 series II GC coupled with a Hewlett-Packard 5971A mass selective detector with helium as a carrier gas). Infrared spectra were taken on a Nicolet 510M FTIR spectrometer. The electronic absorption spectra were recorded on a Shimadzu UV-2101PC UV-visible spectrophotometer or a Hewlett-Packard 8452A Diode Array UV-visible spectrophotometer. The stopped flow experiments were performed on a High Tech Scientific SF-61 instrument coupled to a Czerny-Turner monochromator with a fiber optic cable. C, H, and N analyses were performed by Atlantic Microlab Inc., Norcross, GA. All other elemental analyses were performed by E&R Microanalytical Laboratory, Inc., Corona, NY. For the rate law studies, the temperature was controlled using a Dataplate PMC 720 series digital hot plate/stirrer.

Synthesis of [(C₄H₉)₄N]₈H₂[Co₄(H₂O)₂P₂W₁₈O₆₈] (1). K₁₀[Co₄(H₂O)₂P₂W₁₈O₆₈] (2 g, 0.36 mmol) was dissolved in 50 mL of water with the aid of heat. After the solution was cooled to 30 °C, 1.1 g (3.4 mmol) of tetrabutylammonium bromide was added and the pH was adjusted to 6.5. To the resulting mixture was added 20 mL of CH₂Cl₂ and 10 mL of CH₃CN to form two homogeneous liquid phases, a dark purple heavier organic layer and a nearly colorless lighter aqueous layer. These phases were shaken for 10 min. The deep purple organic layer was concentrated to dryness on a rotary evaporator at 30 °C. The purple solid was redissolved in 3 mL of CH₃CN. Anhydrous diethyl ether (30 mL) was added to this solution to form an oil. The supernatant was decanted off and the oil was treated several times with anhydrous diethyl ether to obtain a fine gray powder. The compound was redissolved in 10 mL of CH₃CN and recrystallized by ether diffusion method at -20 °C. UV-visible (400–800 nm, in acetonitrile) λ , nm (ϵ , M⁻¹ cm⁻¹): 500 (138.3), 525 (sh, 158.5), 570 (186.0). IR (1300–400 cm⁻¹): 1152 (w), 1106 (w), 1062 (m, sh), 1043 (s), 968 (s), 947 (s), 910 (m, sh), 883 (m), 835 (s), 776 (s), 723 (s), 585 (w), 505 (w).

Anal. Calcd for C₁₂₈H₂₉₄Co₄N₈O₇₀P₂W₁₈: C, 23.04; H, 4.44; Co, 3.53; N, 1.68; O, 1.68; P, 0.93; W, 49.59. Found: C, 23.01; H, 4.49; Co, 3.44; N, 1.70; P, 0.91; W, 50.06.

Catalytic Epoxidation Reactions. In a typical reaction, a mixture of **1** (0.001 mmol) and cyclohexene (1 mmol) in 0.5 mL of acetonitrile was thoroughly degassed and purged by argon. The reaction was stirred at 700 rpm and initiated by the addition of a degassed solution of CDMANO (0.1 mmol in 0.5 mL of acetonitrile) under argon. The reaction was quenched by CS₂ before product analysis.⁵⁹ The organic products were analyzed by GC and GC/MS using decane as an internal standard. The footnotes in Tables 2 and 3 give any deviations from these conditions.

Binding Studies. Coordination constants and coordination numbers of 4-picoline *N*-oxide, *N*-methylimidazole, and pyridine to **1** were determined by electronic absorption spectral techniques in acetonitrile at 25 °C.^{60,61} The pertinent equilibria are those in eqs 2 and 3. The



electronic absorption measurements were made on a Shimadzu UV-2101PC UV-visible spectrophotometer equipped with a thermostated cell attached to a circulating constant temperature bath. All the measurements were made with the temperature of the cuvette controlled at 25 ± 1 °C. The spectra were recorded with medium scan speed and a wavelength interval of 0.2 nm per point. Corrections were made for dilution effects, and 10 mm path length quartz cuvettes were used throughout. For each ligand, the volume of ligand added was controlled

(59) Powell, M. F.; Pai, E. F.; Bruce, T. C. *J. Am. Chem. Soc.* **1984**, *106*, 3277–3285.

(60) Connors, K. A. *Binding Constants: The Measurement of Molecular Complex Stability*; John Wiley & Sons: New York, 1987; Chapter 4.

(61) Walker, F. A.; Lo, M.-W.; Ree, M. T. *J. Am. Chem. Soc.* **1976**, *98*, 5552–5560.

to be <25% of the total volume to prevent large deviations resulting from dilution. All stack plots of the spectra with increasing concentration of ligand show nice isosbestic points. A plot of log [(A - A₀)/(A_f - A)] vs log [L] was obtained, where A = the absorbance at a known concentration of L, A₀ = the absorbance in the absence of L, and A_f = the absorbance in the presence of a 100-fold excess of L. The slope of this plot provided the stoichiometry of the complexation of L to the Co complex, and the y intercept provided the binding constants K₁ and β_2 . Curve fits were conducted using the linear fit from Kaleidagraph (version 3.0.1, Synergy Software, Reading, PA) and the errors were calculated using standard error analysis methods.⁶²

UV-Visible Studies of Intermediates in Catalytic Reactions. In a typical reaction, a solution of **1** (0.008 mmol) and cyclohexene (0.99 mmol) in 2 mL of acetonitrile in a Schlenk quartz cuvette was thoroughly degassed and then placed under argon. The solution was stirred at 460 rpm at 25 °C and the reaction initiated by addition of a degassed solution of CDMANO (0.19 mmol in 1 mL of acetonitrile) under argon. The UV-visible spectral changes were followed by a Hewlett-Packard diode array spectrophotometer at wavelengths from 400 to 800 nm. The control reactions were performed with either no cyclohexene or with the dominant CDMANO derived product in the catalytic reactions, *p*-cyano-*N,N*-dimethylaniline (CDMA, 0.99 mmol) in place of cyclohexene. The same concentration of **1** and CDMANO was used for studies of the formation rate of the green adduct by stopped flow technique. After the reaction, the product mixtures were run through a silica gel column. The first fraction was eluted with chloroform and the second fraction was eluted with a 3:1 chloroform-methanol mixture. The polyoxometalate catalysts could be partially removed from the column as a suspension by eluting with methanol. The ¹H NMR and GC-MS confirmed the first fraction from the column to be 95% CDMA. Four lines of evidence given in the Results and Discussion are consistent with the second fraction being a complex mixture of brown oxidation-condensation products derived from the anilines.

Kinetics. All reactions were carried out under argon with deoxygenated solvents. The initial rates V₀ = +{d[epoxide]/dr}_{initial} were evaluated from the rate of epoxide formation at less than 1% conversion. The dependence of rate V₀ on a wide concentration range of [**1**], [CDMANO], and [cyclohexene] was evaluated to define the functional dependence. In a typical reaction, a solution of known concentration of CDMANO in CH₃CN was added to a solution of known concentrations of both **1** and cyclohexene in CH₃CN such that the final volume was 5 mL. The concentration dependence of CDMA was studied at [cyclohexene]₀ = 1.20 M, [CDMANO]₀ = 0.57 M, and [**1**]₀ = 0.002 M. The amount of CDMA added was varied from 0% to 40% of the total CDMANO concentration used in the catalytic reaction. The reactions were stirred at 700 ± 10 rpm at 50 ± 1 °C. At known time intervals, 50- μ L aliquots were removed from the reaction mixture and quenched by 0.2 mL of 50% CS₂ in CH₂Cl₂.⁵⁹ The organic products were identified by GC/MS and quantified by GC using a programmed temperature gradient (50 °C for 3 min, 20 °C/min up to 300 and 300 °C for 6 min). The GC column was calibrated with CH₃CN solutions containing known concentrations of the organic oxidation products using decane as an internal standard. Each quenched reaction mixture was injected three times and an average peak area was used to measure the concentrations of different organic products. Exact concentrations are given in the figure captions.

Results

Alkene Epoxidation by *p*-Cyano-*N,N*-dimethylaniline *N*-Oxide (CDMANO) Catalyzed by d-Electron Transition Metal-Substituted Polyoxotungstates. Tables 1 and 2 give organic product distributions from cyclohexene oxidation catalyzed by six representative TMSP complexes and organic product distributions from oxidation of four different alkenes by the most effective catalyst, **1**, respectively. It is apparent from Table 1 that while the monosubstituted Keggin derivatives [Mn^{III}PW₁₁O₃₉]⁴⁻, [Mn^{II}PW₁₁O₃₉]⁵⁻, [Fe^{III}PW₁₁O₃₉]⁴⁻, and


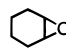
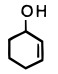
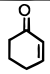



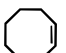
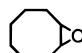
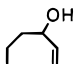
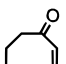
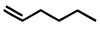
(62) Skoog, D. A. In *Principles of Instrumental Analysis*, 3rd ed.; Saunders College Publishing: Philadelphia, 1985; Chapter 1.

Table 1. Cyclohexene Oxidation by CDMANO Catalyzed by TMSP Complexes

catalyst ^a	[CDMANO] (M)	time (h)	product (%) ^b		
			oxide	enol	enone
[Mn ^{III} PW ₁₁ O ₃₉] ⁴⁻ ^c	0.5	72	0.2	0.5	0.6
[Mn ^{II} PW ₁₁ O ₃₉] ⁵⁻ ^c	0.5	72	<0.1	<0.1	<0.1
[Fe ^{III} PW ₁₁ O ₃₉] ⁴⁻ ^c	0.5	72	<0.1	0.8	<0.1
[NiPW ₁₁ O ₃₉] ⁵⁻ ^c	0.5	72	0.1	<0.1	<0.1
[CoPW ₁₁ O ₃₉] ⁵⁻ ^c	0.5	24	13.1	0.3	0.2
[Co ₄ P ₂ W ₁₈ O ₆₈] ¹⁰⁻ ^c	0.5	16	22.1	0.8	0.4
[Co ₄ P ₂ W ₁₈ O ₆₈] ¹⁰⁻ ^d	0.1	2	17.6	1.2	0.5

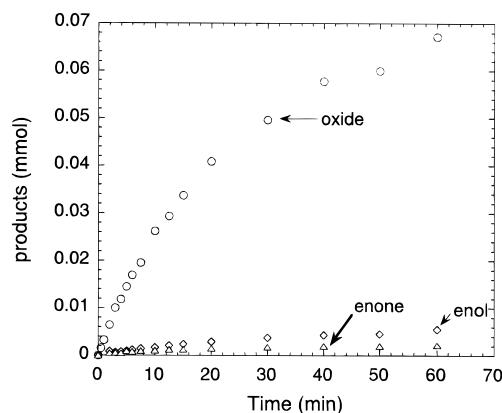
^a All catalysts used are tetrabutylammonium salts (see Experimental Section). ^b Yields are based on the CDMANO amount used. ^c Reaction conditions: 5.00 mM of catalyst and 2.50 M of cyclohexene in 2 mL of acetonitrile at 25 °C under argon. ^d Reaction conditions: 1.00 mM of catalyst and 1.00 M of cyclohexene in 1 mL of acetonitrile at 50 °C under argon.

Table 2. Organic Products from Oxidation of Representative Alkenes with CDMANO Catalyzed by **1**^a

Substrate	Products			
	Selectivity [yield] (turnovers of 1) ^b			
				
	87% [23.7] (22.9)	3% [0.8] (0.7)	5% [1.5] (1.5)	
			PhCHO	
	93% [6.6] (6.3)	c	c	
				
	95% [17.1] (16.5)	c	c	
	c			

^a Reaction conditions: 2 mL of acetonitrile solutions of **1** (0.9 mM), CDMANO (0.09 M), and alkene substrate (0.9 M) were maintained at 50 °C for 2 h under Ar and then quenched by 5 mL of 50% CS₂ in CH₂Cl₂. ^b Selectivity = moles of indicated product/moles of all organic products derived from substrate [yield of product based on total CDMANO added = moles of product/total moles of CDMANO] (turnover = moles of particular organic product/moles of catalyst). ^c No detectable reaction (detection limit <0.2%).

[Ni^{II}PW₁₁O₃₉]⁵⁻ have some reactivity (the catalyst free control indicated no oxidation within the limit of detection, <0.1% yield), they are less selective for epoxide and two orders of magnitude less reactive than the Co complexes, [CoPW₁₁O₃₉]⁵⁻ and **1**. It is apparent from Table 2 that **1** catalyzes CDMANO oxidations of cycloalkenes and stilbenes but not terminal alkenes under these mild reaction conditions (25 or 50 °C in acetonitrile solution). The yields of oxidative cleavage products even for *cis*-stilbene, a substrate vulnerable to this process, were below the detectable limit. A typical time course, that for oxidation of cyclohexene in Figure 2, shows conventional behavior. No induction period or autocatalysis is seen for generation of any of the products. Prior to evaluation of both the rate behavior of these catalytic reactions and the formulation of an overall rate law and mechanism, two tasks are appropriately addressed. First, the association equilibria of **1** with pertinent ligands including a CDMANO model, *N*-methylmorpholine *N*-oxide (MMNO), must be evaluated. MMNO was selected as a model for CDMANO since both are aliphatic tertiary amine *N*-oxides and both are known to be susceptible to catalytic transfer of oxygen to organic substrates by soluble transition metal

**Figure 2.** Time-dependent yields of the oxidation products from reaction of 1.00 M cyclohexene with 0.100 M CDMANO catalyzed by 1.00 mM **1** in 1.0 mL of acetonitrile under Ar at 50 °C.

complexes.^{38,40,41,44–46,59,63} Second, the various spectroscopically observable intermediates during these catalytic reactions must be examined.

Equilibrium Association Constants Involving **1.** Substantial data on a variety of homogeneous oxo transfer oxidations of organic substrates catalyzed by metalloporphyrins and other d-electron transition metal complexes are consistent with an association of the oxygen donor with the transition metal center prior to substrate oxygenation.^{64–70} Furthermore, such pre-association with concomitant activation of the oxygen donor is clearly operable in the CDMANO/**1** epoxidation system as consumption of CDMANO takes place in the absence of alkene (the deoxygenation product of oxidant, CDMA, is formed). The association number and constants could be readily determined spectrophotometrically and the data are of high quality and reproducible. Figure 3 illustrates the association of pyridine and **1**; isosbestic behavior and a 12-point fit with a linear correlation coefficient of 99.9% are obtained. Ligand binding to **1** more than likely involves displacement of a solvent molecule on Co^{II} and not ligation to five-coordinate Co^{II}. Coordinately unsaturated five-coordinate Co^{II} in O₅ polyoxo-metalate ligation polyhedra of comparable charge density have been well studied and both five-coordinate Co^{II} and Co^{III} have substantially different spectral properties than six-coordinate Co^{II}.⁷¹ Bromide can be ruled out as a potential sixth ligand from the elemental analysis of the isolated forms of **1** (<0.2% Br) and from the quality of the binding data. While the association constants, *K*₁ and β₂, for CDMANO to **1** (eqs 2 and 3) could not be readily determined as this combination led to immediate subsequent reaction, the association of MMNO and other nitrogen bases could be determined under conditions very similar to or the same as those of the actual catalysis. However, no oxo transfer reactivity was noted for the *N*-oxides other than CDMANO as indicated by no significant change in the UV–visible spectra for a long period of time. These association

(63) Brown, R. B.; Williamson, M. M.; Hill, C. L. *Inorg. Chem.* **1987**, *26*, 1602.

(64) Meunier, B. *Chem. Rev.* **1992**, *92*, 1411–1456.

(65) McMurry, T. J.; Groves, J. T. In *Cytochrome P-450*; Ortiz de Montellano, P. R., Ed.; Plenum: New York, 1986; Chapter 1.

(66) Ortiz de Montellano, P. R. In *Cytochrome P-450*; Ortiz de Montellano, P. R., Ed.; Plenum: New York, 1986; Chapter 7.

(67) Ostovic, D.; Bruce, T. C. *Acc. Chem. Res.* **1992**, *25*, 314–320.

(68) Yang, Y.; Diederich, F.; Valentine, J. S. *J. Am. Chem. Soc.* **1991**, *113*, 7195–7205.

(69) Mansuy, D. *Pure Appl. Chem.* **1987**, *59*, 759–770.

(70) Mansuy, D.; Battioni, P. In *Activation and Functionalization of Alkanes*; Hill, C. L., Ed.; Wiley: New York, 1989; pp 195–218.

(71) Katsoulis, D. E.; Pope, M. T. *J. Am. Chem. Soc.* **1984**, *106*, 2737–2738.

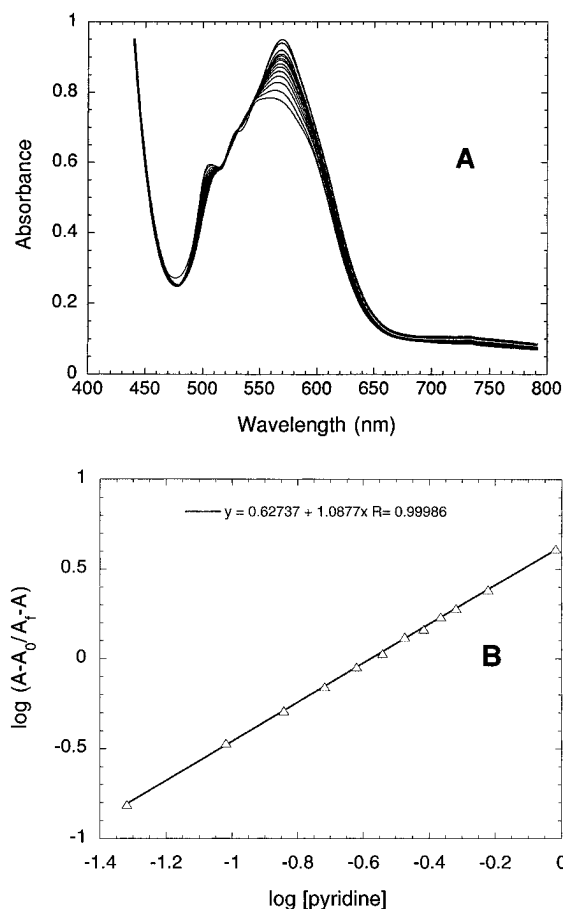


Figure 3. (A) Stacked plot of visible spectral changes after addition of pyridine to 4.0×10^{-3} M of **1** in acetonitrile at 25 °C. (B) Analysis of absorbance change at 568 nm upon addition of pyridine to a solution of **1**

Table 3. Binding Constants for Addition of Amines to **1** in Acetonitrile at 25 °C

ligand	K_1, M^{-1}	β_2, M^{-2}
<i>N</i> -methylimidazole	275 ± 13	$(1.07 \pm 0.05) \times 10^4$
pyridine	4.3 ± 0.1	<i>a</i>
4-picoline <i>N</i> -oxide	59 ± 3	<i>a</i>
4-cyanopyridine <i>N</i> -oxide	22 ± 1	<i>a</i>
<i>N</i> -methylmorpholine <i>N</i> -oxide	57 ± 5	<i>a</i>
4-cyano- <i>N,N</i> -dimethylaniline	<i>b</i>	<i>b</i>

^a Not obtainable from analysis (see Results and Discussion). ^b No detectable binding up to [CDMA]/[**1**] of 100 to 1.

constants are given in Table 3 and both the experimental details and theory are outlined in the Experimental Section. Solubility limitations and/or low association constant values prohibited determination of β_2 except in the case of *N*-methylimidazole. CDMA exhibited no detectable binding to **1** at up to 100 equiv per equivalent of **1**. The relative binding strengths of the ligands are in agreement with both their relative basicity and steric bulk. It is clear that 1:1 but not 2:1 complexes of the *N*-oxides with **1** are relevant under the conditions of catalysis in these studies.

UV–Visible Studies of Intermediates and Products. When CDMAO is added to a mixture of **1** and cyclohexene, the initial purple solution due to **1** immediately turns green. As the green solution stands, the UV–visible absorption in the 400–650-nm region increases, and in several hours a brown solution results. The stack plot of absorption change vs time was obtained (Figure S2, supporting information). These UV–visible spectral changes, in theory, would provide the spectroscopy evidence for the decay and the formation of any relative long-lived intermediates or products. Examination of the spectra

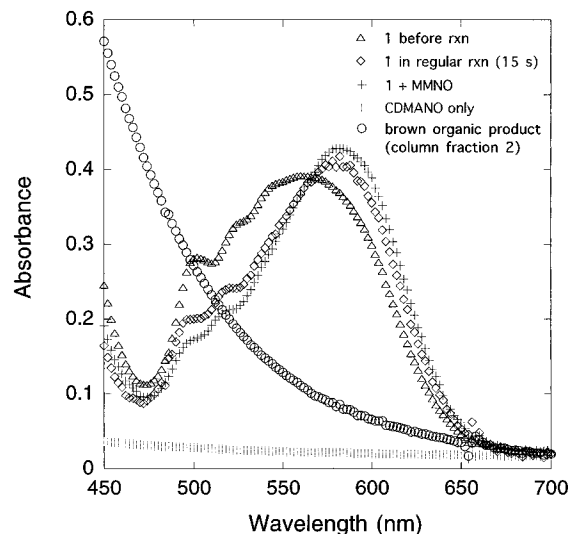


Figure 4. Electronic absorption spectra (450–700 nm) of species directly pertinent to the catalysis: the catalyst, **1**, before reaction, the reaction itself at $t = 15$ s (**1** with CDMAO and cyclohexene, 25 °C under Ar), **1** with MMNO, CDMAO alone, and the second fraction eluted from the product purification column after the catalytic reaction. The various spectra are indicated by the legend insert in the order above.

of several species including the final brown material after chromatographic isolation provides useful information on the identities of these chromophores. However, quantitative deconvolution of the different species was not possible in this case (Figure S3, supporting information). Two species were clearly identified, namely the adduct between **1** and CDMAO and the brown material. Figure 4 shows the electronic absorption spectra of **1** prior to addition of CDMAO, CDMAO alone, **1** with MMNO (the CDMAO model), the catalytic reaction of **1** with CDMAO and cyclohexene after a reaction time of 15 s, and the second eluent isolated from a silica gel column after the catalytic reaction of **1** with CDMAO and cyclohexene that contains much of the final brown chromophore. The spectrum of the green intermediate species under catalytic conditions (**1**, CDMAO, and alkene) resembles the spectrum of the green adduct of **1** and MMNO fairly closely. Both green species have a shifted absorption maximum at 495 (sh), 520 (sh), and 580 nm as compared to the purple color of **1** prior to addition of *N*-oxide with absorbances at 500, 525, and 570 nm. These data coupled with the binding data suggest that the green color generated at the initial stage of the reaction is the 1:1 adduct of CDMAO and **1**. The formation of this adduct is a very rapid process. Assessment of the formation rate of this adduct by stopped-flow techniques indicate a pseudo-first-order rate constant $> 10^3$ s⁻¹. All of the data are consistent with the pre-equilibrium association of CDMAO and **1**.

The final brown chromophore was chromatographically separated from the CDMAO derived aniline, CDMA, and independently examined (see Experimental Section for details). Four lines of evidence are consistent with the isolated brown material being oxidation–condensation products derived from the anilines. Such products are ubiquitous in heterocyclic chemistry, particularly from transformations of such compounds under aerobic conditions. First, the ¹H NMR has a complex pattern in both the aromatic (6–9 ppm) and aliphatic (1–3 ppm) regions. Second, the electronic absorption spectrum is featureless with a very long tail into the visible imparting the typical brown color. Third, the material is high boiling and polar (none of it traverses the nonpolar GC column indicated above after 20 min at 300 °C), and fourth, control reactions with CDMA as the substrate in the regular catalytic reaction in place of

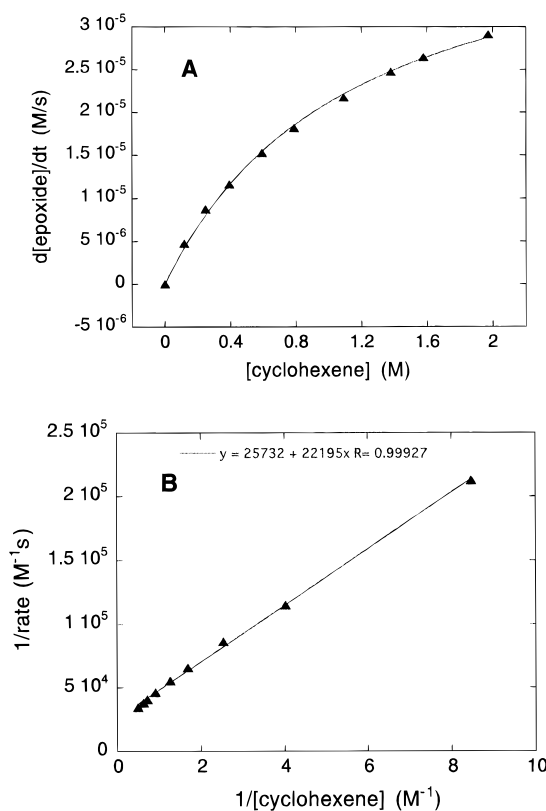


Figure 5. (A) Rate vs concentration of cyclohexene plot illustrating the complex functional dependence of rate on the concentration of cyclohexene. (B) Lineweaver–Burk plot of the inverse rate vs the inverse concentration of cyclohexene. For (A) and (B), $[1] = 2.22$ mM, $[CDMANO] = 0.0566$ M, and the concentration of cyclohexene was varied from 0.118 to 1.97 M; reactions were run under argon at 50 °C.

cyclohexene result in a substantial increase of these complex brown polar aromatic products. It is noted that there was no significant difference in the UV–visible absorption spectra of the products from reaction of **1** with CDMANO only and the products from reaction of **1** with CDMANO and cyclohexene at longer reaction times (≥ 1 h). Furthermore, the quantity of brown material from reaction of **1** with CDMANO and CDMA was greater at all reaction times than that from reaction of **1** with CDMANO only or **1** with CDMANO and cyclohexene. Unfortunately, absorbance interference by the brown organic products prevented further detailed kinetic studies of the decay of the 1:1 CDMANO–**1** adduct or the formation of other possible catalyst intermediates.

Rate Law and Mechanism. The rate law for a representative reaction, the epoxidation of cyclohexene by CDMANO catalyzed by **1** (acetonitrile; 50 °C), has been evaluated. The rates were determined over a suitably wide range of concentrations of cyclohexene substrate, CDMANO, and **1**. The cyclohexene substrate concentration dependence was determined with $[1] = 2.22$ mM and $[CDMANO] = 0.0566$ M while the concentration of cyclohexene was varied from 0.118 to 1.97 M. Figure 5A plots the rate of epoxide formation versus the concentration of cyclohexene and illustrates the complex functional dependence of the rate on cyclohexene concentration. Figure 5B is a Lineweaver–Burk plot (inverse rate versus inverse substrate concentration) of the same data. The reactions exhibit apparent Michaelis–Menten kinetics behavior. The CDMANO oxidant functional dependence was evaluated with $[1] = 2.22$ mM, $[cyclohexene] = 1.10$ M, while the concentration of CDMANO was varied from 0.0114 to 0.165 M. Figure 6 plots these data in an analogous manner to that in Figure 5 for the substrate.

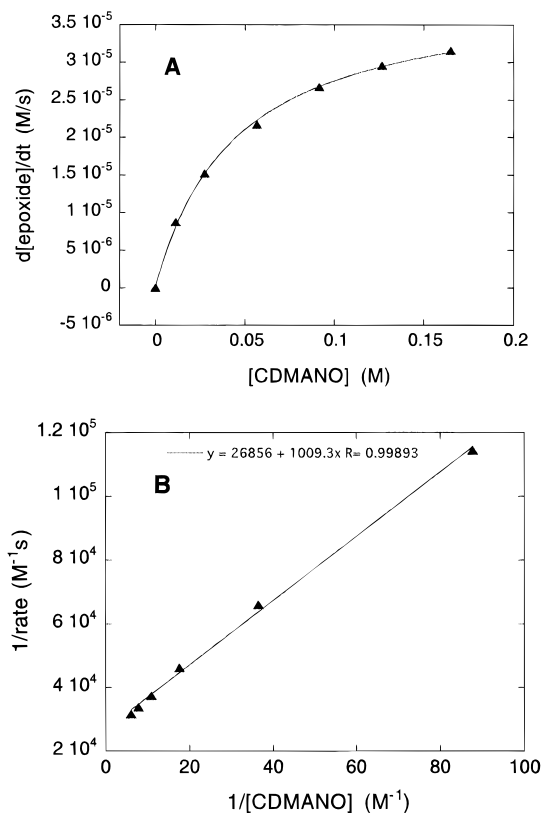


Figure 6. (A) Rate vs concentration of CDMANO plot illustrating the complex functional dependence of rate on the concentration of CDMANO. (B) Lineweaver–Burk plot of the inverse rate vs the inverse concentration of CDMANO. For (A) and (B), $[1] = 2.22$ mM, $[cyclohexene] = 1.10$ M, and the concentrations of CDMANO were varied from 0.0114 to 0.165 M; reactions were run under argon at 50 °C.

Figure 7 plots the functional dependence of the reaction on **1**. Measurements were carried out with $[CDMANO] = 0.0566$ M, $[cyclohexene] = 1.10$ M while $[1]$ was varied from 0.624 to 3.92 mM. The complicated empirical rate law is given in eq 4 (Figure S4, supporting information):

$$d[\text{epoxide}]/dt = \frac{k'[\text{cyclohexene}][\text{CDMANO}][\text{Co}_4\text{P}_2\text{W}_{18}\text{O}_{68}^{10-}]_T}{\{k''[\text{CDMANO}] + k'''[\text{cyclohexene}] + k''''[\text{cyclohexene}][\text{CDMANO}] + k'''''\}} \quad (4)$$

The effect of CDMA on the rate of epoxidation has also been assessed. The experiments were carried out with $[CDMANO] = 0.0566$ M, $[cyclohexene] = 1.20$ M, and $[1] = 0.0022$ M while the concentration of CDMA was varied from 0% to 40% of the total CDMANO concentration used. The data indicate clearly that an increase in CDMA concentration results in a decrease in the epoxidation rate (Figure S5, supporting information).

Discussion

A number of mechanisms for this reaction can be ruled out. Trivially, direct reaction between the cyclohexene substrate and the CDMANO oxidant can be ruled out as both species are soluble and there is no detectable reaction in the absence of the catalyst, **1**. Mechanisms involving reaction between alkene complexed to **1** (activated by **1**) are unlikely. UV–visible spectral properties of **1** at high concentrations of alkene in acetonitrile closely resemble those of **1** in the absence of alkene indicating no significant association between alkene and **1**. In

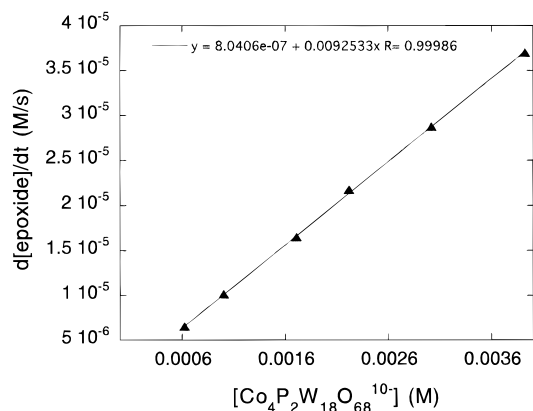
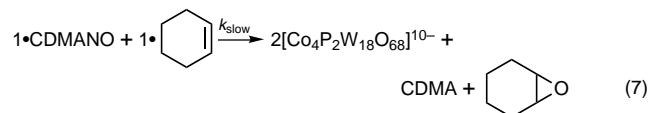
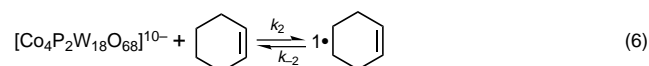
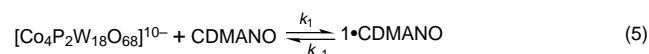
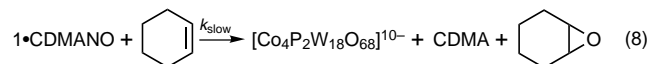
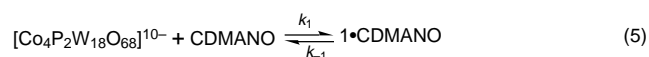


Figure 7. Initial rate of cyclohexene epoxidation as a function of **1**. $[\text{CDMANO}] = 0.0566 \text{ M}$, $[\text{cyclohexene}] = 1.10 \text{ M}$, and concentration of **1** was varied from 0.624 to 3.92 mM; reactions were run under argon at 50 °C.

Scheme 1



Scheme 2



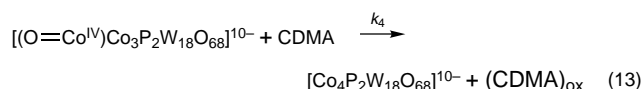
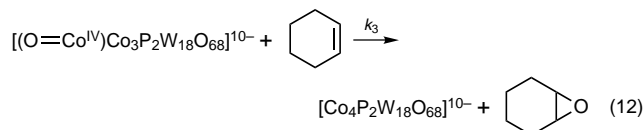
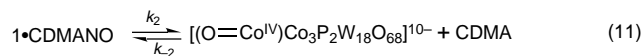
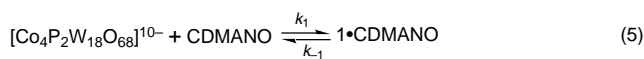
$$\frac{d[\text{epoxide}]}{dt} = \frac{K_1 k_2 [\text{cyclohexene}] [\text{CDMANO}] [\text{Co}_4\text{P}_2\text{W}_{18}\text{O}_{68}^{10-}]_T}{K_1 [\text{CDMANO}] + 1} \quad (9)$$

$$\frac{d[\text{epoxide}]}{dt} = \frac{k_1 k_2 [\text{cyclohexene}] [\text{CDMANO}] [\text{Co}_4\text{P}_2\text{W}_{18}\text{O}_{68}^{10-}]_T}{k_1 [\text{CDMANO}] + k_{-1} + k_2 [\text{cyclohexene}]} \quad (10)$$

addition there are no literature examples, to the best of our knowledge, of association between alkene and Co^{II} ions in such conventional “hard” ligand environments and there is no evidence for significant kinetic activation of alkene with respect to oxygenation by such complexes. Complexations of CDMANO to species like **1** with consequent activation of the *N*-oxide, however, are well established.^{38–46} Reaction between two pre-equilibrium adducts, 1:1 CDMANO–**1** (henceforth **1**•CDMANO) and alkene–**1**, Scheme 1, can be ruled out as this requires a rate law second order in **1**. Another possibility is saturation of both olefin and CDMANO at a single Co site. This is highly unlikely. A third possible mechanism involves saturation of one Co site in one complex by olefin and at a second Co site in the same complex by CDMANO. This molecular arrangement, however, does not defensibly lie along the reaction coordinate for epoxidation which demands that both olefin and oxidant be in proximity.

The most likely mechanisms for cyclohexene oxygenation by CDMANO catalyzed by **1**, based on the very substantial literature for homogeneous transition metal-catalyzed oxygenation, are given in Schemes 2 and 3. In the rate law derived for Scheme 2, eq 9, the following reasonable assumptions are made. First, the total concentration of **1** is distributed between the original form and the **1**•CDMANO, and second, k_1/k_{-1} constitutes an equilibrium. This rate law, eq 9, is not compatible

Scheme 3



$$\frac{d[\text{epoxide}]}{dt} = \frac{K_1 k_2 k_3 [\text{cy}][\text{ox}][\text{Co}_4\text{P}_2\text{W}_{18}\text{O}_{68}^{10-}]_T}{K_1 k_2 [\text{ox}] + k_3 [\text{cy}] + K_1 k_3 [\text{cy}][\text{ox}] + (k_{-2} + k_4)[\text{an}] + K_1 (k_{-2} + k_4)[\text{an}][\text{ox}]} \quad (14)$$

cy = cyclohexene; ox = CDMANO; an = CDMA

with the kinetics data, and in particular is inconsistent with the cyclohexene dependence. When **1**•CDMANO is treated as the catalytic intermediate, the rate law eq 10 can be derived from Scheme 2. The curve fit to the kinetics data using eq 10 yields a k_1 of $\sim 20 \text{ M}^{-1} \text{ s}^{-1}$. This is inconsistent with the direct measurement of the adduct formation rate, k_1 , by stopped flow techniques ($k_1 > 10^4 \text{ M}^{-1} \text{ s}^{-1}$). The value of k_1 is not surprising given the rate of H_2O substitution in $[\text{Co}(\text{H}_2\text{O})_6]^{2+}$ ($k \sim 5 \times 10^6 \text{ s}^{-1}$).⁷² The lower symmetry of the CoO_6 coordination polyhedron in **1**•CDMANO ($\sim C_{4v}$) relative to that in $[\text{Co}(\text{H}_2\text{O})_6]^{2+}$ ($\sim O_h$) would more than likely lead to an even faster rate of ligand exchange on the former relative to the latter primarily as the loss of ligand field stabilization energy on going to the transition state is lower in the case of **1**•CDMANO. Furthermore, two additional lines of evidence are inconsistent with Scheme 2. First, the product distributions in Table 2 are typical of those generated by reaction with *unhindered* high-valent oxometal species ($\text{O}=\text{M}$ ($\text{M} = \text{Fe}^{\text{IV}}$ or $\text{Mn}^{\text{IV,V}}$) in literature studies^{64,67} and a $\text{O}=\text{Co}^{\text{IV}}$ in this study). In contrast, direct oxygenation by the highly sterically hindered **1**•CDMANO would doubtless yield a significantly different product distribution. Second, T. C. Bruice and co-workers in their thorough mechanistic evaluation of hydrocarbon oxygenation by CDMANO catalyzed by Mn and Fe porphyrins concluded that oxygenation does not take place by *N*-oxide adducts of the metals but by high-valent oxometal intermediates.^{38–46} Finally, there is no evidence in the literature, to the best of our knowledge, for an *N*-oxide adduct of a transition metal functioning as the species responsible for transferring oxygen to another molecule.

Scheme 3 in contrast to Scheme 2 involves formation of and oxygenation of substrate by a high-valent oxo species. While reactive oxo– Co^{IV} species are not as common as the corresponding high-valent oxo forms of Fe, Mn, and some other mid-transition metals, they are nonetheless documented.^{73,74} Application of the steady state approximation to the oxo– Co^{IV} intermediate in Scheme 3 yields the rate law in eq 14 (Figure S6, supporting information). This is consistent with the experimental rate law eq 4 derived from the kinetics studies. The epoxidation rate decreases when an increasing amount of authentic CDMA was added to reactions with fixed concentra-

(72) Merbach, A. E. In *Inorganic High Pressure Chemistry*; van Eldik, R., Ed.; Elsevier: Amsterdam, 1986; p 70.

(73) Koola, J. D.; Kochi, J. K. *J. Org. Chem.* **1987**, *52*, 4545–4553.

(74) Jørgensen, K. A. *Chem. Rev.* **1989**, *89*, 431–458.

tions of other reagents (Figure S5, supporting information). The oxidation reaction with CDMANO has similar UV–visible absorption spectra in the presence and absence of substrate cyclohexene. All these data point to the fact that at higher conversion, the oxidant-derived oxidation product, CDMA, can compete with cyclohexene as a substrate for the reactive form of the catalyst.⁷⁵

In summary, the title catalytic alkene oxygenation system is selective and rapid. The present work represents the most detailed kinetic study of a TMSP-catalyzed oxygenation reaction to date. The considerable mechanism parallels between homogeneous oxygenation reactions catalyzed by metalloporphyrins versus those catalyzed by TMSP complexes, based in part on this research, further define TMSP complexes to be defensible oxidatively resistant analogs of metalloporphyrins.

(75) One of the three referees suggested that the complex alkene dependence might be explained by this scenario, namely, a conversion dependent competition between alkene and oxidant derived oxidation products for the reactive intermediate form of the catalyst. We thank the reviewer for this suggestion.

Acknowledgment. This research was supported by the National Science Foundation (Grant No. CHE-9412465). We thank Dr. Alex Khenkin and Dr. Dong Hou for Figures 1A and 1B, respectively.

Supporting Information Available: Figures showing an example of the initial rate determination, stack plot of absorbance change vs time, difference spectra of Figure S2, experimentally determined rate law, effect of CDMA on the rate of epoxidation, derivation of the theoretical rate law for Scheme 3, and raw kinetics data (9 pages). This material is contained in many libraries on microfiche, immediately follows this article in the microfilm version of the journal, can be ordered from the ACS, and can be downloaded from the Internet; see any current masthead page for ordering information and Internet access instructions.

JA9536983